

CONF-770401--22

April 30, 1977

ANL/FPP/TM-81

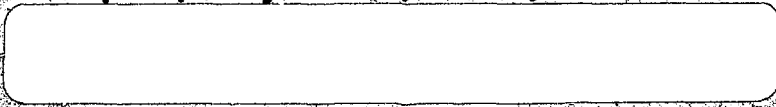
**IMPORTANT ASPECTS OF RADIATION SHIELDING
FOR FUSION REACTOR TOKAMAKS**

Mohamed A. Abdou

*Applied Physics Division
Argonne National Laboratory
Argonne, Illinois 60439*

ANL/FPP TECHNICAL MEMORANDUM NO. 81

**Results reported in the FPP series of memoranda
frequently are preliminary and subject to revision.**



Approved for release by the U. S. Energy Research Administration

CONFIDENTIAL

IMPORTANT ASPECTS OF RADIATION SHIELDING FOR FUSION REACTOR TOKAMAKS

Mohamed A. Abdou

*Applied Physics Division
Argonne National Laboratory
Argonne, Illinois 60439*

NOTICE
This report was prepared as an account of work sponsored by the United States Government. Neither the United States nor the United States Energy Research and Development Administration, nor any of their employees, nor any of their contractors, subcontractors, or their employees, makes any warranty, express or implied, or assumes any legal liability or responsibility for the accuracy, completeness or usefulness of any information, apparatus, product or process disclosed, or represents that its use would not infringe privately owned rights.

ABSTRACT

Radiation shielding is a key subsystem in tokamak reactors. Design of this shield must evolve from economic and technological trade-off studies that account for the strong interrelations among the various components of the reactor system. These trade-offs are examined for the bulk shield on the inner side of the torus and for the special shields of major penetrations. Results derived are applicable for a large class of tokamak-type reactors.

I. INTRODUCTION

A very notable characteristic of a tokamak reactor is a strong and complex interface among a large number of subsystems. Radiation shielding is a key subsystem that plays a major role in defining this complex interface. Shielding in tokamaks presents a new set of interesting and challenging problems above and beyond those familiar in other shielding applications. The primary purpose of this paper is to delineate some of these problems, and discuss some of the possible solutions.

The shield system in a tokamak reactor power plant consists of several components: (1) first wall/blanket; (2) primary bulk shield; (3) penetration shield; and (4) biological shield. Figure 1 shows a vertical cross section in a tokamak reactor that demonstrates the physical relationship between the shield components and other reactor subsystems. The first wall is surrounded by the blanket. The primary function of the blanket is to convert the kinetic energy of fusion neutrons and secondary gamma rays into heat. In reactors operated on the DT cycle, choice of materials in the blanket is limited to lithium in one form or another in order to provide the necessary tritium regeneration. The primary bulk shield circumscribes the blanket. The basic function of the primary shield is radiation protection of reactor components, particularly the toroidal field (TF) coils as detailed later. The blanket/bulk shield subsystem is required to accommodate a variety of penetrations. Penetration shields provide for protection against radiation streaming from penetrations. In the expected regime for reactor operation, the radiation biological dose outside the reactor is several orders of magnitude higher than the maximum permissible dose for occupationally exposed individuals. Therefore, a biological shield is necessary. It is conceived that the walls of the reactor building can serve the dual purpose of providing the necessary containment as well as biological shielding.

The two most critical problems in tokamak shielding are addressed in this paper. Section II deals with the constraints on the design of the shield on the inner side of the torus. The effects of major penetrations and the design of special penetration shields are addressed in Sec. III.

II. INNER SHIELD

One of the strongest interactions between the shield subsystem and the entire reactor system concerns the attenuation requirements on and the thickness of the primary shield on the inner side of the torus. The incentive to conserve on the space on the inner side of the torus comes primarily from three reasons:

- (1) The reactor thermal power, P_T , varies with Δ_{BS}^i as

$$P_T \sim \left(1 - \frac{r_w + \Delta_{BS}^i}{R}\right)^4 B_m^4,$$

where R is the plasma major radius, r_w is the first-wall radius, B_m is the maximum toroidal magnetic field at the inner coil winding, and Δ_{BS}^i is the distance in midplane from the first wall to the TF coil windings. The largest portion of Δ_{BS}^i is occupied by the inner blanket/shield but it also includes maintenance clearance space, and the dewar, thermal and magnetic shield, and bobbin of the TF coils. The cost of the TF coils increases as $\sim B_m^2$ and the maximum practical value of B_m is limited by technological constraints. The above equation shows that a very significant increase in the reactor power is obtainable by reducing Δ_{BS}^i .

(2) For the same R , r_w , B_t , and P_T reducing Δ_{BS}^i reduces B_m and Δ_m , and increases r_v where Δ_m is the thickness of the TF coil (and its support structure) and r_v is the central core radius ($r_v = R - r_w - \Delta_{BS} - \Delta_m$). Increasing r_v reduces the ohmic heating field, B_{OH} . Besides the technological constraints on B_{OH} , the cost of the OH coils, and more importantly the cost of the power supply increases rapidly with B_{OH} .

(3) Plasma confinement improves with the magnetic field at the plasma centerline, B_t . These factors provide a very strong incentive to reduce Δ_{BS}^i . Satisfying the energy conversion and tritium breeding requirements in the blanket and providing the radiation attenuation in the blanket/shield necessary for magnet protection favors a relatively large Δ_{BS}^i . Therefore, a prudent tokamak reactor design must be optimized as to the requirements on and utilization of the space on the inner side of the torus. These requirements are discussed next, followed by a brief examination of the optimization problem.

The requirement of tritium breeding in the blanket necessitates the use of a lithium-containing material in the blanket. Employing natural lithium causes $\sim 20\%$ increase in Δ_{BS}^i compared with an all stainless steel blanket. Two solutions are possible:

(1) The volume of the inner portion of the blanket is only $\sim 10\%$ of the total volume. Calculations with present data indicate that it is feasible to achieve a breeding ratio, T , greater than 1.0 without employing any lithium in the inner portion of the blanket.

(2) If the previous solution does not prove feasible, then only a thin ($\sim 2-5$ cm) layer of lithium highly enriched in ^6Li can be employed in the inner blanket. High breeding ratios are then attainable with a minor or no increase in Δ_{BS}^1 .

The primary shielding functions of the blanket/shield subsystem are:

(1) To reduce the nuclear heating in the TF coils to the levels allowed by (a) total power required to run the refrigerators; and (b) maximum local heating rates imposed by practical limits for coil design.

(2) To attenuate the nuclear radiation to the levels allowed by tolerable radiation damage to the components of the superconducting magnet. These components are (a) the superconductor; (b) the normal (stabilizing) conductor; (c) electrical and thermal insulators; and (d) structure.

It is of great interest to find out which of these requirements is more limiting on the blanket/shield design. To show this we have selected a blanket of 30 cm stainless steel followed by 50% stainless steel + 50% B_4C shield. The thickness of the shield was varied and the effect on the TF coils was examined. Figures 2-6 show the results. It should be noted that Δ_{BS}^1 in all these figures include provision for 10% of the volume as void to account for a variety of cooling, clearance, and other engineering requirements in addition to a fixed 5-cm vacuum gap generally required in the TF coils for thermal insulation.

Figure 2 shows the maximum volumetric nuclear heating rate in the TF coils as a function of Δ_{BS}^1 for two values of the neutron wall loading, P_w , 1 MW/m^2 and 10 MW/m^2 , covering the attractive practical range for tokamak operation. Superconducting magnets are generally designed to accommodate a nonnuclear heat load of ~ 0.5 to 1.0 MW/m^3 (W/cm^3). A nuclear heat load of 0.01 MW/m^3 is therefore a small increment that can be easily accommodated in a practical magnet design. From Fig. 2, the minimum Δ_{BS}^1 is 0.68 and 0.84 m for P_w of 1.0 and 10 MW/m^2 , respectively. The total electric power required to run the refrigerator expressed as a fraction, f_{re} , of the plant electric power output is shown also in Fig. 2. The parameter f_{re} is insensitive to P_w . The limit on f_{re} is an economics question. Figure 3 shows two curves. Curve a is the thermal power as a function of Δ_{BS}^1 for a reactor with $R = 8$ m and an aspect ratio, A , of 2.5. Curve b shows the dependence on Δ_{BS}^1 of the net thermal power, i.e. the gross thermal power minus the refrigeration power requirements. The maximum power occurs at $\Delta_{\text{BS}}^1 \sim 0.91$ m. The value of Δ_{BS}^1 corresponding to maximum power is not overly sensitive to R but it strongly depends on the attenuation efficiency of the shield. Figures 2 and 3 show that net power (economics) considerations are more limiting on how small Δ_{BS}^1 is than the local heating limits. This is an important conclusion as it suggests that additional optimization can be made to further reduce Δ_{BS}^1 while simultaneously increasing the outer shield thickness to keep the total refrigeration power to a reasonable level. It should be noted also that the optimum f_{re} here is $\sim 1.5\%$, a factor of 15 higher than the limit on refrigeration power suggested earlier in the literature.

Irradiation of superconductors causes² generally a decrease in the critical current density, J_c . A reduction in J_c requires an increase in the amount of the superconductor to keep the operational current the same. Radiation damage to the superconductor can be recovered by near-room temperature. The annealing of the magnet requires $\sim 2-3$ months of plant

downtime. Therefore, economic tradeoffs among Δ_{BS}^i , operational current density, and frequency of annealing are apparent. Figure 4 shows the maximum neutron fluence in a NbTi superconductor as a function Δ_{BS}^i for $I_w = 1$ and 30 MW-yr/m^2 where I_w , integral neutron wall loading, is the product of P_w and an operational time period, t_0 . The value of t_0 here corresponds to the time span between magnet anneals. Three experimental points for the reduction in J_c as a function of neutron fluence, ϕt , are shown in the figure. At $\phi t \sim 3 \times 10^{22} \text{ n/m}^2$, $\Delta J/J_c = -10\%$. At higher fluences, the reduction in J_c becomes very large. A minimum Δ_{BS}^i at 1 MW-yr/m^2 is $\sim 0.8 \text{ m}$ to limit $\Delta J/J_c$ to $\sim 10\%$, the optimum value if damage to the superconductor was the only radiation effect in the magnet.

Irradiation of normal conductor at low temperatures causes an increase in the electrical resistivity. A near complete recovery of the radiation-induced resistivity is obtainable by magnet anneal. The variation of the radiation-induced resistivity, p_r , in copper with Δ_{BS}^i is shown in Fig. 5 for $I_w = 1$ and 30 MW-yr/m^2 . The optimum value of p_r can be obtained only from a tradeoff study for the particular reactor design considered. If all other radiation effects in the magnet were neglected, a typical optimum value for p_r is found to be near $3 \times 10^{-8} \Omega\text{-cm}$. At this value $\Delta_{BS}^i = 0.9 \text{ m}$ for $I_w = 1 \text{ MW-yr/m}^2$ and $\Delta_{BS}^i = 1.15 \text{ m}$ for $I_w = 30 \text{ MW-yr/m}^2$.

Superconducting magnets employ a variety of electrical and thermal insulations. Organic insulators are believed to be necessary for large magnets since inorganic insulators are very brittle. There is a serious lack of irradiation data on insulators at low temperature.³ It is known, however, that organic insulators are much less resistant to radiation damage than inorganic insulators. Furthermore, radiation damage in these insulators is irreversible. Therefore, the insulators in the TF coils must be designed to function properly for the lifetime of the plant, typically $\sim 30 \text{ yr}$. Figure 6 shows the maximum dose in the TF coil insulators as a function of Δ_{BS}^i at 30 and 300 MW-yr/m^2 . Extrapolation of neutron irradiation data suggests dose limits of $\sim 10^8$ rad and $\sim 10^9$ to 5×10^9 rad for mylar and epoxy base insulators, respectively. (Regions indicated by the letters M and E in Fig. 6.) Thus, the minimum Δ_{BS}^i is ~ 1.0 - 1.3 m for epoxy and ~ 1.28 - 1.48 for mylar. Region I in Fig. 6 shows that with radiation damage limits on inorganic insulators of $\sim 10^{12}$ to 5×10^{12} rad, the minimum Δ_{BS}^i is ~ 0.5 to 0.8 m .

Since inorganic insulators are very brittle, it seems at present that organic insulators with their low threshold to radiation damage have to be used. From Figs. 4-6, at $I_w = 30 \text{ MW-yr/m}^2$, the required Δ_{BS}^i set by superconductor, stabilizer, and insulators are 1.04 , 1.15 , and 1.02 m , respectively. If no annealing were possible for the superconductor and stabilizer, their requirements would be more limiting than those of the insulators. However, since radiation damage to superconductors and normal conductors can be recovered while radiation damage to organic insulators is irreversible, it is apparent that radiation attenuation requirements of the organic insulators are more demanding on the minimum Δ_{BS}^i than all other effects in the TF coils.

An important conclusion to be made from the results in this section is that the design of the inner shield in terms of material composition and thickness must evolve from a trade-off study for the particular system. A system program⁴ for fusion power plants at ANL has built-in capabilities for performing this type of trade-off studies. Table 1 shows an

Table 1. Effect of Inner Blanket/Shield Thickness on Cost of Energy Production^a

Δ_{BS}^i (m)	P_w (MW/m ²)	Cost of Energy (Mills/kwh)	Dose to Insulator at End of Plant Life, 30 yr (rad)
0.75	9.5	31	2×10^{12}
1.0	8.0	24	5×10^{10}
1.25	6.8	26	2×10^9
1.5	5.6	28	4×10^8

^aBased on noncircular plasma with $B_m = 8$ T, $A = 2.5$, and vanadium-base alloy for structure.

example of the dependence of the energy production cost on Δ_{BS}^i for a tokamak reactor with $B_m = 8$ T, $A = 2.5$, and vanadium-base alloy for structural material. The blanket/shield material composition is similar to that discussed earlier (SS/SS-B₄C). The minimum cost occurs with $\Delta_{BS}^i \sim 1$ m. These results assumed that insulators at a typical cost can last for the lifetime (30 yr) of the plant. The last column in Table 1 shows the dose in insulators at the end of 30-yr operation. It is seen from this table that ductile insulators that can stand 10^{10} - 10^{12} rads need to be developed. Insulator limits of 10^8 - 10^9 rads require an increase in Δ_{BS}^i beyond the optimum value with a significant economic penalty in the cost of power and the cost of energy production. If normal TF coils are to be employed instead of superconducting magnets, the desirable radiation dose limits on insulators are even higher.

III. OUTER BULK SHIELD AND PENETRATION SHIELDING

In the previous section, the severe constraints on the space available for the bulk shield on the inner side of the torus were examined. The problem of space for shielding on the top, bottom, and outer side of the torus is somewhat different. The bores of the TF coils can be expanded vertically and horizontally to the outside without compromising the performance of the reactor or imposing new requirements for technological developments. Therefore, the bulk shield in these regions can, in principle, be constructed with materials that meet many other desirable criteria. There are two strong incentives, however, to improve radiation attenuation and reduce the thicknesses of the top, bottom, and outer regions of the bulk shield. The first incentive comes from the fact that extending the horizontal and vertical bores of the TF coils causes an increase in the dimensions and hence the cost of the TF coils, the reactor containment building, and heat transport system (piping). The second incentive concerns penetration effects discussed below.

Tokamak reactors require that the blanket/shield system accommodates normal and major penetrations, including those for vacuum pumping, auxiliary heating [e.g. neutral beam, radio frequency (rf), etc.], divertor and maintenance access. Many of these penetrations are large open regions

which extend from the first wall radially outward through the blanket/shield and between the TF coils. These penetrations are numerous and large and they can be accommodated only on the top, bottom, and outer regions of the shield. The bulk shield does very little to prevent radiation streaming through these penetrations and special penetration shields have to be provided. The penetrations and their special shields create a space problem inside and inbetween the TF coils.

A study has been undertaken recently at ANL to quantify radiation streaming of penetrations and to examine possible shielding approaches.⁵ Penetration effects and their neutronics treatment depend on considerable engineering details that vary significantly from one reactor design to another. The purpose of this paper, however, is to examine the general aspects of radiation shielding that are common to tokamak reactors. Therefore, subsection A below is devoted to a discussion of the generic problems of penetration effects and possible shielding approaches. Computational models for penetrations are examined in subsection B.

A. Penetration Effects and Shielding Approach

The geometric arrangement of a typical major penetration is shown in Figs. 1 and 7. The entire reactor (torus) consists of a number (typically 12 to 20) of repeating segments each similar to that in Fig. 7. This type of configuration was examined employing the continuous energy Monte Carlo code VIM and some of the important results are shown in Table 2 for several cases. Case 1 has no penetration. A penetration with circular cross section that has a diameter of 0.2 m, 0.42 m, and 0.85 m was employed in cases 2, 3, and 4, respectively. Case 5 is to be discussed shortly. Three important parameters that characterize neutron streaming effects are shown in the table. These are the maximum neutron flux in the TF coils, the maximum flux inside the duct and exterior to the TF coils, (i.e. maximum neutron flux in zone 25 shown in Fig. 7), and the total neutron leakage through a toroidal surface that is in the immediate exterior of the TF coils. The statistical error (i.e. the standard deviation) on the values in Table 2 varies from ~10% for the large ducts to ~50% in the smaller ducts.

Table 2. Some Neutronics Effects of Penetrations

Case No.:	1	2	3	4	5
Diameter of duct (m)	0.0	0.2	0.42	0.85	0.85
Shield ^b (m)	—	0.0	0.0	0.0	0.70
Maximum flux at TF coils ^a (n/cm ² -sec)	1.0(8)	1.1(10)	3.5(11)	4.1(12)	1.3(8)
Maximum flux in the duct region outside the TF coils ^a (n/cm ² -sec)	1.0(8)	5.4(11)	4.3(12)	1.2(13)	9.9(12)
Leakage per DT neutron	1.2(-6)	8.3(-5)	1.2(-3)	2.0(-2)	4.0(-3)
Maximum heating ^a in beam injector (W/cm ³)	—	5.0(-4)	4.0(-2)	1.5(-1)	1.2(-1)

^aNormalized to a neutron wall load of 1 MW/m².

^bThickness of duct shield.

The results in Table 2 show that streaming from penetrations is very significant and requires provision for additional shielding. The results show that the neutron leakage per source neutron is roughly equal to the square of the ratio of the penetration cross-sectional area to the area of the first wall. Thus, for the same reactor, reducing the size of a penetration decreases radiation streaming in proportion to the square of the penetration cross-sectional area. These results are derived only for penetrations with circular cross sections. It remains to be seen yet how the width-to-height ratio of a rectangular cross section would affect radiation streaming.

There are several approaches for shielding against penetration effects. For those penetrations that do not need to be open during the plasma burn, a logical approach is to employ a movable shield plug that closes the penetration completely at all times when the fusion probability is greater than zero. The vacuum pumping ducts represent an example of this type. The design and operation of a heavy movable shield plug involves several engineering problems. However, it seems that such a movable shield plug presents the least-challenging design problems at present. The functional requirements of other types of ducts such as those for divertor and neutral beams in a beam-driven device, necessitates that these ducts be open during the plasma burn. For this type of penetrations, a local exterior penetration shield that surrounds the penetration as it emerges from the bulk shield seems to be the only viable approach. Several important questions need to be addressed concerning the design of this penetration shield. Some of these questions relate to the material composition and dimensions of the penetration shield and also the impact of penetrations on the design of the bulk shield.

Our studies on penetrations resulted in defining the following guidelines for a cost-effective shielding approach: (1) for a given material composition, the dimensions of the bulk shield should be kept to the minimum that is sufficient to protect the TF coils in the complete absence of any penetration effects; (2) the penetration shield must reduce the maximum radiation level at the TF coils and the poloidal coils to that in the absence of penetrations; and (3) the local exterior penetration shield must also extend far enough to protect auxiliary systems external to the TF coils that are affected by penetration-assisted streaming.

Case 5 in Table 2 shows the neutron fluxes and leakages when a 0.85 m diameter duct is completely surrounded by a 0.7 m thick local penetration shield of SS-B₄C. Comparing the results for this case with those of case 1 (no penetration) shows that this local shield is barely adequate to protect the TF coils. The thickness, t , of the penetration shield required to protect the TF coils depends on both penetration shield material composition and the tolerable radiation level at the coils. For a large class of typical reactors, the required t is comparable to the duct diameter.

In addition to protection of the magnets, penetration shields together with the bulk shield must provide for protection of all other reactor components and equipment located outside the TF coils. Two problems are of particular concern. The first problem concerns radiation streaming into the beam injectors. A local exterior penetration shield can protect components on the sides of the beam duct but it has a very poor efficiency for attenuation of radiation streaming into the beam injector (typically a factor of three reduction per meter parallel to the beam duct axis for $d = 0.5$ m).

Cryopumping has been suggested as the most favorable mode for beam injector vacuum pumping. The nuclear heating rate in the cryopanel for a typical system at 1 MW/m^2 neutron wall load is 0.1 and 0.05 W/cm^3 for a 0.85 m and 0.4 m beam ducts, respectively as shown in Table 2. A large area of cryopanel is always required and these high heating rates cast some doubt on the practical as well as economical use of cryopumping in the neutral beam lines. Since the beam ducts have to provide a straight-through path from the first wall to the injector, shielding of components inside the beam injector is extremely difficult. A recent study at ANL showed that a zirconium-aluminum pump⁶ may be a viable alternative to cryopumping. Available irradiation data show no significant deterioration in pumping speeds up to $\sim 10^{27} \text{ n/m}^2$ in a fission spectrum. Therefore, zirconium-aluminum pumps can be operated successfully in the beam injectors for the lifetime of the machine.

Practical considerations require that the level of induced activation in air (or any other gas) inside the reactor containment building be kept to a manageable level. In addition, there is an economic incentive to reduce the radiation level outside the TF coils to a low level such that the induced activation within relatively short time (1-2 days) after shut-down does not prevent personnel access to the reactor building. Calculations indicate that in the absence of penetrations, the bulk shield can properly be designed to satisfy these requirements. Radiation streaming through the beam injectors increases the radiation level in the reactor building by two to four orders of magnitude (see Table 2). Therefore, surrounding the large size beam injectors with a shield becomes necessary to meet these requirements. The use of a shield plug in the beam duct, however, could possibly eliminate the need for an additional shielding around the beam injectors, depending on the exact reactor design.

Penetrations in the blanket and bulk shield cause many additional problems that cannot be covered here. Eliminating unnecessary penetrations and reducing the size of the required penetrations must be a serious design objective. Accomplishing this goal involves many technical and engineering areas in addition to neutronics. An example of possible improvements in design concepts can be demonstrated by examining the evacuation ducts. Reactor studies in the past required these evacuation ducts to extend to the first wall. A recent study⁶ for EPR at ANL showed that vacuum pumping can be accomplished by evacuation ducts that are connected to the beam ducts at locations outside the shield as shown in Fig. 1. This concept has several advantages over the use of separate ducts that extend directly to the first wall.

B. Multidimensional Calculational Models

The impact of penetrations in tokamaks is so strong that they must be treated as an integral part of the early phases of the reactor design. Multidimensional transport calculations are required for neutronics treatment of penetrations. The development of efficient models for geometric representation and nuclear analysis of penetrations is, therefore, necessary. In the course of this study, three models were examined:

(1) Full three-dimensional model: In this model all the geometric details of the reactor are included. Toroidal geometry becomes an important factor in this model. Engineering details of tokamaks, however, show that toroidal surfaces with circular or elliptical cross sections are not important and in many cases are undesirable approximation. (See,

for example, Fig. 1.) Representation of the torus cross section depends on the particular reactor design. Monte Carlo is the only viable method for this type of three-dimensional geometry.

(2) An approximate three-dimensional model: In this model, toroidal geometry is ignored and only one repeating segment of the reactor (see Fig. 7) is considered.⁵ Of particular importance in this model is the proper representation of the TF coils so as to reproduce the correct spacing between the TF coils relative to the penetrations.

(3) An approximate two-dimensional model: This model can be considered for a major penetration where the interest is in characterizing the radiation field inside and in the vicinity of the penetration.⁷ The geometric model consists basically of a set of concentric cylinders with the penetration axis as the common axis. In (r,z) coordinates, the origin is at the plasma geometric center, and the z-axis is taken along the common axis. This model although approximate has two clear advantages. The first is a substantial saving in computational time, compared with three-dimensional calculations, which makes it attractive for scoping studies. Another advantage is the feasibility of obtaining a deterministic solution to the transport equation by employing the S_n method.

Computational time required to obtain a solution for a given accuracy depends strongly on the geometry and engineering details of the system and particularly the size of penetrations. Case 4 (0.85 m diameter duct) in Table 2 required 20,000 histories for a standard deviation in the TF coil flux of $\sim 9\%$ while case 2 (0.2 m diameter duct) resulted in a standard deviation of $\sim 55\%$ after 50,000 histories were run.

ACKNOWLEDGMENT

The author thanks Dr. W. M. Stacey, Jr. and Dr. J. Jung of Argonne National Laboratory for many fruitful discussions. This work was supported by the U. S. Energy Research and Development Administration.

REFERENCES

1. M. A. Abdou and C. W. Maynard, "Nuclear Design of the Magnet Shield for Fusion Reactors," p. 685, Proc. First Top. Mtg. Technology of Controlled Nuclear Fusion, USAEC CONF-740402-P1 (1974).
2. B. S. Brown, "Radiation Effects on Superconductivity," p. 330, in Radiation Damage in Metals, N. L. Peterson and S. D. Harkness, Editors, American Society of Metals, 1975.
3. C. A. M. Van der Kulin, "The Organic Insulators in Fusion Reactor Magnet Systems," Reactor Centrum Nederland, RCN-240 (1975).
4. M. A. Abdou, et al., "Impact of Major Design Parameters on Economics of Tokamak Power Plants," Trans. Am. Nucl. Soc. 25 (June 1977).
5. M. A. Abdou, et al., "Multidimensional Neutronics Analysis of Major Penetrations in Tokamaks," p. 845, Proc. Sec. ANS Top. Mtg. Tech. of Controlled Nuclear Fusion, USERDA CONF-760935-P3 (1976).
6. W. M. Stacey, Jr., et al. "EPR-77, A Revised Design for the Tokamak Experimental Power Reactor," ANL/FPP/TM-77 (1977).
7. J. Jung and M. Abdou, "A Two-Dimensional Neutronics Model for Major Penetrations in Tokamaks," Trans. Am. Nucl. Soc. 25 (June 1977).

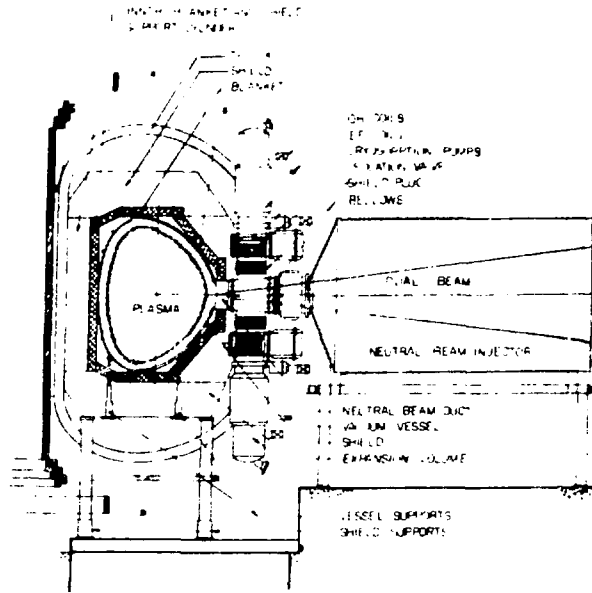


Fig. 1. A Vertical Cross Section of a Tokamak

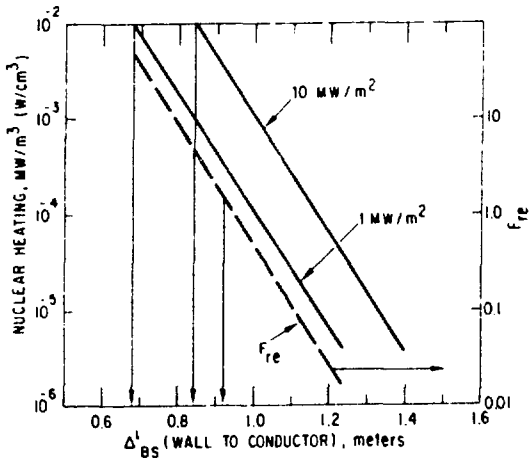


Fig. 2. Variation of the Maximum Heating and f_{re} in TFC with Δ_{BS}^1 .

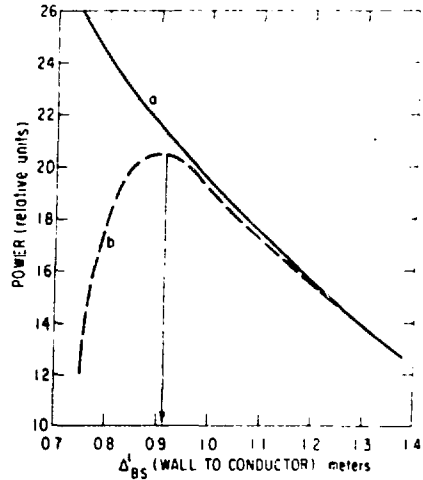


Fig. 3. Variation of (a) Gross Thermal Power; and (b) Gross Thermal Power Minus Refrigeration Power with Δ_{BS}^1 .

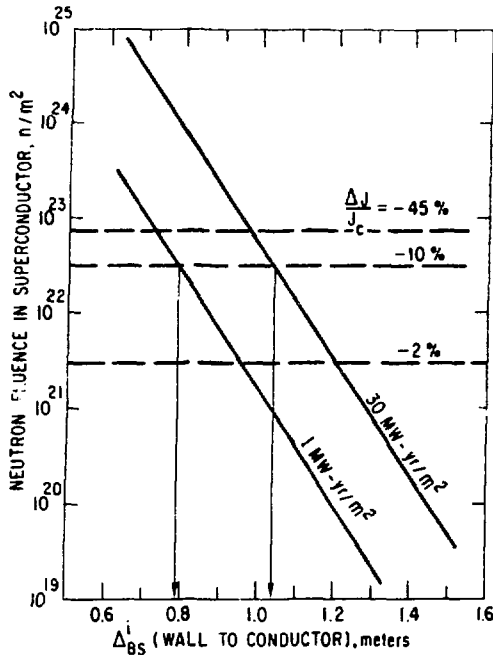


Fig. 4. Maximum Neutron Fluence in TFC Versus Δ_{BS}^i .

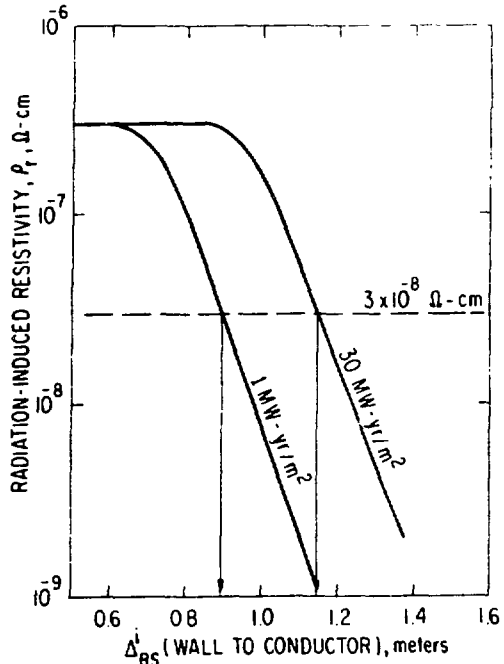


Fig. 5. Maximum Radiation-Induced Resistivity, ρ_r , as a Function of Δ_{BS}^i .

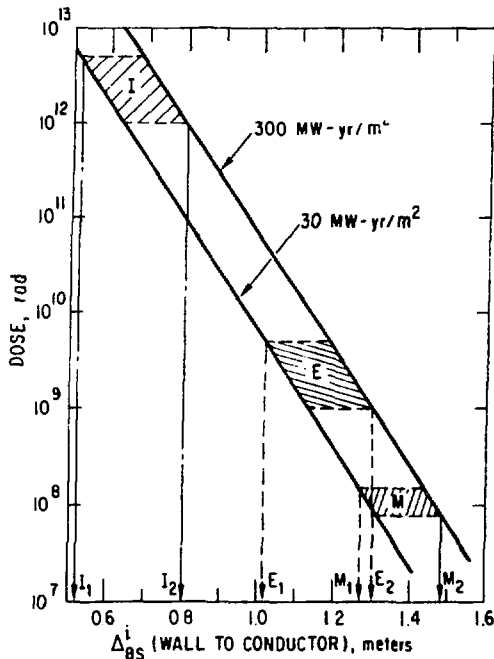


Fig. 6. Variation of Dose in TFC Insulators with Δ_{BS}^i .

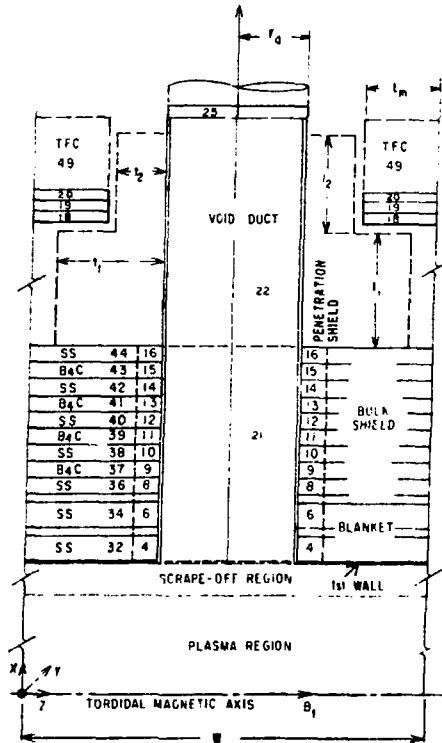


Fig. 7. A Schematic of a Reactor Section with Penetration.